

The Effect of Metastable Level Populations on the Ionization Fraction of Li-like ions

J.G. Doyle¹, H.P. Summers² and P. Bryans²

¹ Armagh Observatory, College Hill, Armagh, BT61 9DG, N. Ireland

² Department of Physics, University of Strathclyde, Glasgow, Scotland

Received date, accepted date

Abstract. Lines from Li-like ions have been known to produce theoretical intensities under-estimated compared to lines of a similar formation temperature. Here we investigate this anomalous behaviour whereby the ionization fractions are calculated using the ADAS code considering the electron density dependence of dielectronic recombination coupled with collisional ionization from metastable levels. For the lines investigated, the line contribution functions show a clear dependence with increasing electron density. For example, C IV 1548 Å shows over a factor of three enhancement for $N_e = 10^{12} \text{ cm}^{-3}$. The increase in the higher temperature lines is lower, but are still in the range of 30 to 60%. Furthermore, all the lines have their peak contribution shifted to lower temperature. Calculating the total radiative power output at an electron density of 10^{11} cm^{-3} , we find that the difference in the transition region is 10–15% while above 10^6 K the difference is around 30% compared to the low density value.

Key words. Sun: atmosphere – Di-electronic Recombination – metastable levels – contribution function – electron density – line intensity – UV/EUV radiation

1. Introduction

The analysis of UV and EUV lines is essential for a proper understanding of high temperature plasma, *e.g.* that found in the upper solar/stellar atmospheres. Data from spectrographs aboard the Solar Heliospheric Observatory (SoHO) has led to a wealth of observations of small-scale dynamic events observed from the Sun's chromosphere to the transition region and corona. On the stellar side, data from the International Ultraviolet Explorer (IUE), Space Telescope Imaging Spectrograph (STIS/HST) and the Far Ultraviolet Spectroscopic Explorer (FUSE) have all provided high quality data which have been used to diagnose properties of the atmospheres in a range of objects. Interpretation of this data is highly dependent on many atomic physics parameters, one of these being the ionization fractions of the ion under consideration (see Young et al. 2003 for a discussion of some of these within the CHIANTI database).

It has been known for many years that lines from Li-like ions can in some instances give very different results from other isoelectronic sequences. Following on from work by Burgess & Summers (1969), Vernazza & Raymond (1979) showed that a significant increase in intensity can occur at high electron densities if one considers electron density dependent dielectronic recombination. In the vast majority of published ionization fractions, the low-density assumption is used, and there-

fore use of these calculations to produce a differential emission measure (DEM) curve using a range of lines including Li-like ions can produce discrepant results (Doyle & Raymond 1984), Del Zanna et al. 2003). In many instances, due to the limitation in the number of available spectral lines from IUE data, emission measure curves for stellar atmospheres have been derived based on data from Li-like ions, *e.g.* C IV 1548/50, N V 1328/42, etc.

The usual practice when considering atomic processes in high-temperature, low-density plasmas, such as discussed here, is to adopt the coronal approximation. This treats the populations of excited states of ions via an excitation balance of collisional excitation, usually from the ground state, by electrons, and radiative decay. The ionization state is established as a balance of electron impact ionization from the ground state and radiative plus dielectronic recombination. In the simplest version of such modelling, secondary collisions with excited states are neglected.

However, there is no consistent treatment of metastable states with populations comparable to the ground state. Thus, in the coronal limit, ionization and excitation balance are independent of electron density. Here we look again into this problem and in particular construct line contribution functions, and then calculate the percentage increase in the line flux for a range of lines. In addition, we calculate the percentage change in the radiative loss function as a result of changes in the electron density.

Send offprint requests to: J.G. Doyle, email: jgd@arm.ac.uk OR <http://star.arm.ac.uk/preprints/>

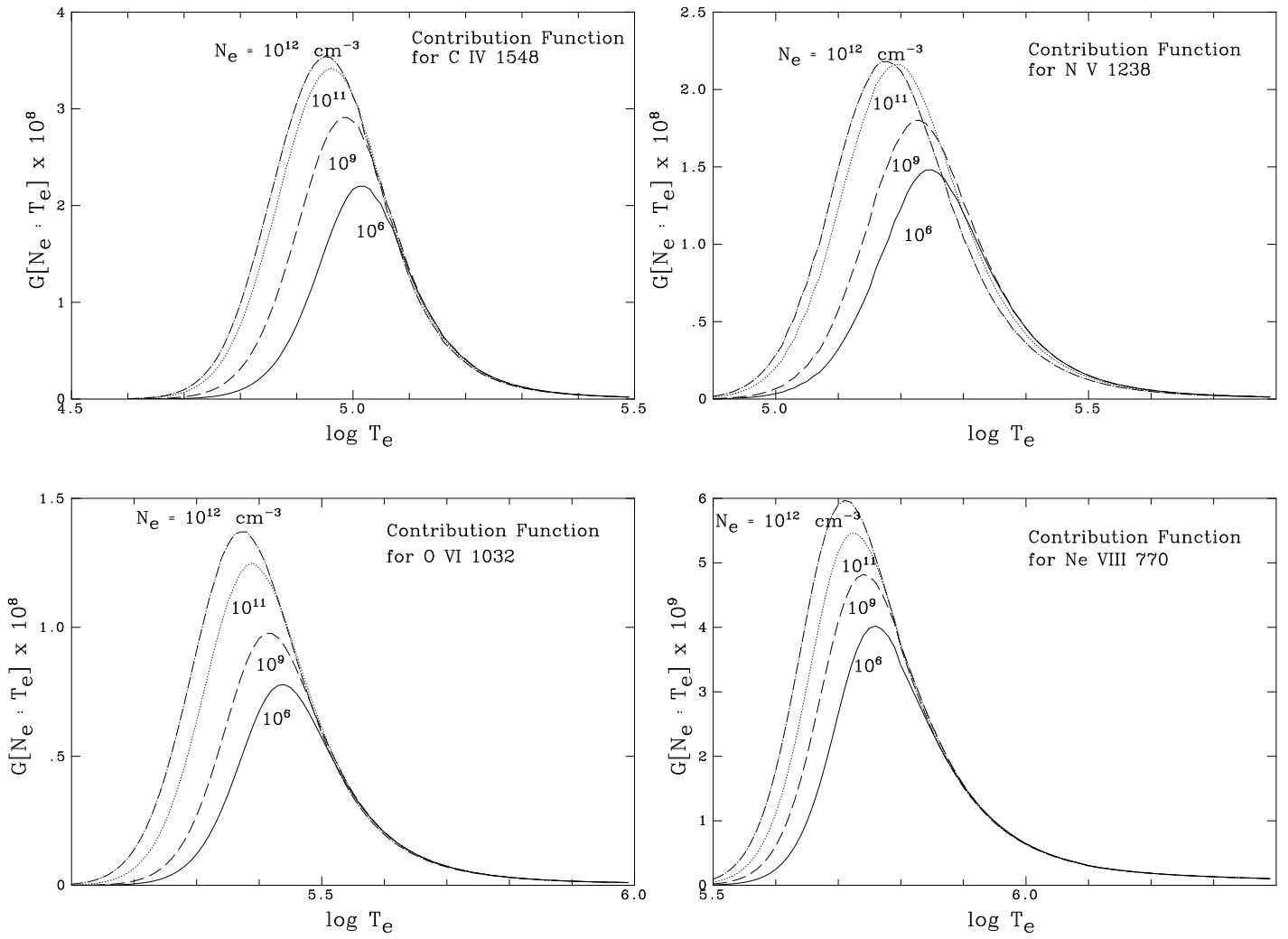


Fig. 1. The contribution function for C IV 1548 Å, N V 1238 Å, O VI 1032 Å and Ne VIII 770 Å line in units of $\text{cm}^3 \text{s}^{-1}$ for four values of the electron density, 10^6 cm^{-3} , 10^9 cm^{-3} , 10^{11} cm^{-3} and 10^{12} cm^{-3} .

2. Atomic Background

The present work aims to determine what effect the full density-dependence of the excitation and ionization balance, including the full role of low-lying metastables, has on emission from Li-like ions in the solar corona. The generalized collisional-radiative picture (GCR; Summers & Hooper, 1983), which builds on the collisional-radiative theory of Bates, Kingston & McWhirter (1962), allows such an analysis. In detail, the collisional ionization and redistribution processes from excited states, ignored in the coronal model, are included. The populated metastable states are determined via an elaborated ionization balance along with the ground states.

If one denotes metastable states (including the ground state) by Greek indices and excited states by Roman indices then the sum of transition rates between states can be represented by the collisional-radiative matrix, C . Such a matrix contains elements $C_{\rho\sigma+}$ and $C_{i\sigma+}$, denoting the sum of the recombination rates from each metastable; $C_{\rho\sigma-}$ and $C_{i\sigma-}$, denoting ionization rates; and diagonal elements $C_{\rho\rho}$ and C_{ii} , indicating total loss

rates from the levels ρ and i . Considering metastable level populations to be dynamic and excited levels to be quasi-static, one can form population equations for each $N_{\rho}^{(z)}$ and $N_i^{(z)}$ in terms of these matrix elements as

$$\frac{dN_{\rho}^{(z)}}{dt} = C_{\rho\sigma}N_{\sigma}^{(z)} + C_{\rho j}N_j^{(z)} + C_{\rho\sigma+}N_{\sigma+}^{(z+1)} + C_{\rho\sigma-}N_{\sigma-}^{(z-1)} \quad (1)$$

$$0 = C_{i\sigma}N_{\sigma}^{(z)} + C_{ij}N_j^{(z)} + C_{i\sigma+}N_{\sigma+}^{(z+1)} + C_{i\sigma-}N_{\sigma-}^{(z-1)} \quad (2)$$

Elimination of the excited populations via the quasi-static assumption leads to the collisional-radiative coefficients, which couple metastables of the ionisation stage of interest to adjacent stages and are the basis of our solution.

There is no significantly populated metastable in the case of Li-like ions, but the metastable resolved picture matters when considering recombination and ionization to and from the He-like and Be-like stages. The variation due to the inclusion of dielectronic recombination is particularly pronounced in the collisional-radiative recombination coefficient. The density dependence of this process makes it of interest here. Collisional

ionization out of excited states suppresses the effect of dielectronic recombination at higher density.

The generalized collisional-radiative coefficients are computed within the Atomic Data and Analysis Structure (ADAS; Summers 2004) framework. ADAS is a collection of fundamental and derived atomic data, and codes that manipulate them. The data are organized in a form that allows generation of the collisional-radiative matrix, which is manipulated to form the derived effective recombination and ionization coefficients.

Starting with the equation for a spectral line, we have the intensity from upper level j to lower level i , integrated over path length h , given by

$$I_{j \rightarrow i} = h\nu_{j \rightarrow i} \int A_{j \rightarrow i} N_j dh \quad (3)$$

where N_j denotes the population density of ions in the upper state j and $A_{j \rightarrow i}$ is the radiative transition probability.

Using the collisional-radiative matrix as described by equations 1 and 2, and making the substitution

$$A_{j \rightarrow i} N_j = \frac{N_{tot}}{N_H} N_e^2 G(T_e, N_e) \quad (4)$$

one can determine $G(T_e, N_e)$ from the populations and transition probabilities. $G(T_e, N_e)$ is known as the density dependent contribution function and corresponds to the well-known $G(T_e)$ function (see Lanzafame et al. 2002). It includes the equilibrium ionisation balance, which in this case is density-dependent metastable resolved. These were calculated for four lines from Li-like ions, namely, C iv 1548 Å, N v 1238 Å, O vi 1032 Å and Ne VIII 770 Å, the results of which are given in the next section.

3. Results

3.1. Contribution Function

Four values of the electron density; 10^6 cm^{-3} for the low density limit, and 10^9 cm^{-3} for a typical quiet Sun electron density, 10^{11} cm^{-3} an active region and 10^{12} cm^{-3} for a flare were used with the results shown in Fig. 1. For these plots we used a temperature spacing of $\log T_e = 0.1$. Here we clearly see that with increasing N_e , the $G(T_e, N_e)$ function shows a significant increase. Furthermore, all the lines have their peak contribution shifted to lower temperature. Folding in the Raymond & Doyle (1981) DEM, we obtain for C iv 1548 Å, a 60% enhancement for $N_e = 10^9 \text{ cm}^{-3}$, leading to over a factor of three enhancement for $N_e = 10^{12} \text{ cm}^{-3}$. The increase is lower for the higher temperature lines, but are still in the range of 30 to 60% larger.

3.2. Radiative Loss Function

With exception of results by Landi & Landini (1999), all other published radiative loss functions were calculated in the low-density limit. From the above population solution, the total radiative power function is calculated as

$$P_{rad} = \sum_{z=0}^{z_0} \sum_{\rho=1}^{M_z} [P_{LT,\rho}^{(z)} + P_{RB,\rho}^{(z)} + (N_H/N_e) P_{RC,\rho}^{(z)}] (N_\rho^{(z)}/N_{tot}) \quad (5)$$

Table 1. The enhancement factor for the intensities of four lines from Li-like ions relative to the low-density value at $N_e = 10^6 \text{ cm}^{-3}$

Line	$N_e = 10^6$	$N_e = 10^9$	$N_e = 10^{11}$	$N_e = 10^{12}$
C iv 1548	1.00	1.59	2.93	3.45
N v 1238	1.00	1.17	1.38	1.37
O vi 1032	1.00	1.28	1.52	1.59
Ne VIII 770	1.00	1.14	1.27	1.30

with contributions arising from low level line power (P_{LT}), recombination-bremsstrahlung-cascade power (P_{RB}) and charge exchange recombination power (P_{RC}). In Fig. 2, we show the percentage difference

$$Diff = \frac{P_{rad}(T_e, N_e = 10^6) - P_{rad}(T_e, N_e^i)}{P_{rad}(T_e, N_e = 10^6)} \quad (6)$$

where $N_e^i = 10^9, 10^{10}, 10^{11} \text{ cm}^{-3}$. In the transition region the difference is 10–20% while above 10^6 K the difference is around 30%. Elements included in the calculation were H, He, C, N, O, Ne, Si, S, Ar, Fe & Ni, i.e. the most abundant elements at these temperatures. Although the detail in Fig. 2 is slightly different from that of Landi & Landini (1999), the general result is similar. However, these differences are small and well within the errors in the atomic data. As pointed out by Landi & Landini, larger differences can arise from an incorrect treatment of the level populations, or the use of different ionization fractions. However, the largest variation is due to abundance.

4. Discussion

The DEM analysis has been an important tool in the study of solar and stellar plasma over the past few decades. However, such an analysis can be suspect if the selection of lines are affected by opacity, inaccurate atomic coefficients (Lanzafame et al. 2002), or inappropriate assumptions concerning the calculation of the ionization fractions (Vernazza & Raymond 1979). A general DEM-rule is that only resonance-type lines (therefore eliminating the electron density dependence) should be used, and since lines from Li-like ions are strong resonance lines these have been used by many authors. This however ignores the density dependence resulting from adjacent ionization stages.

Doyle & Raymond (1983) noted that N v and, to a lesser extent, O vi implied much larger values for the emission measure during the early stages of a large solar flare. For N v this amounted to a factor of 2 to 3. The present results goes a long way to correcting this with perhaps the remaining difference being due to temporal variability (i.e. there was a 2 min. time difference between the observation of the N v and the O v lines used in that particular study). From the results presented in the previous section, assuming that the low-density limit applies to Li-like ions leads to errors of up to factors of 2–3. It is therefore clear that these lines should not be used unless the ionization balance is treated with the necessary physics.

The inclusion of the density dependence in the total power loss has some effect, particularly in the upper transition region,

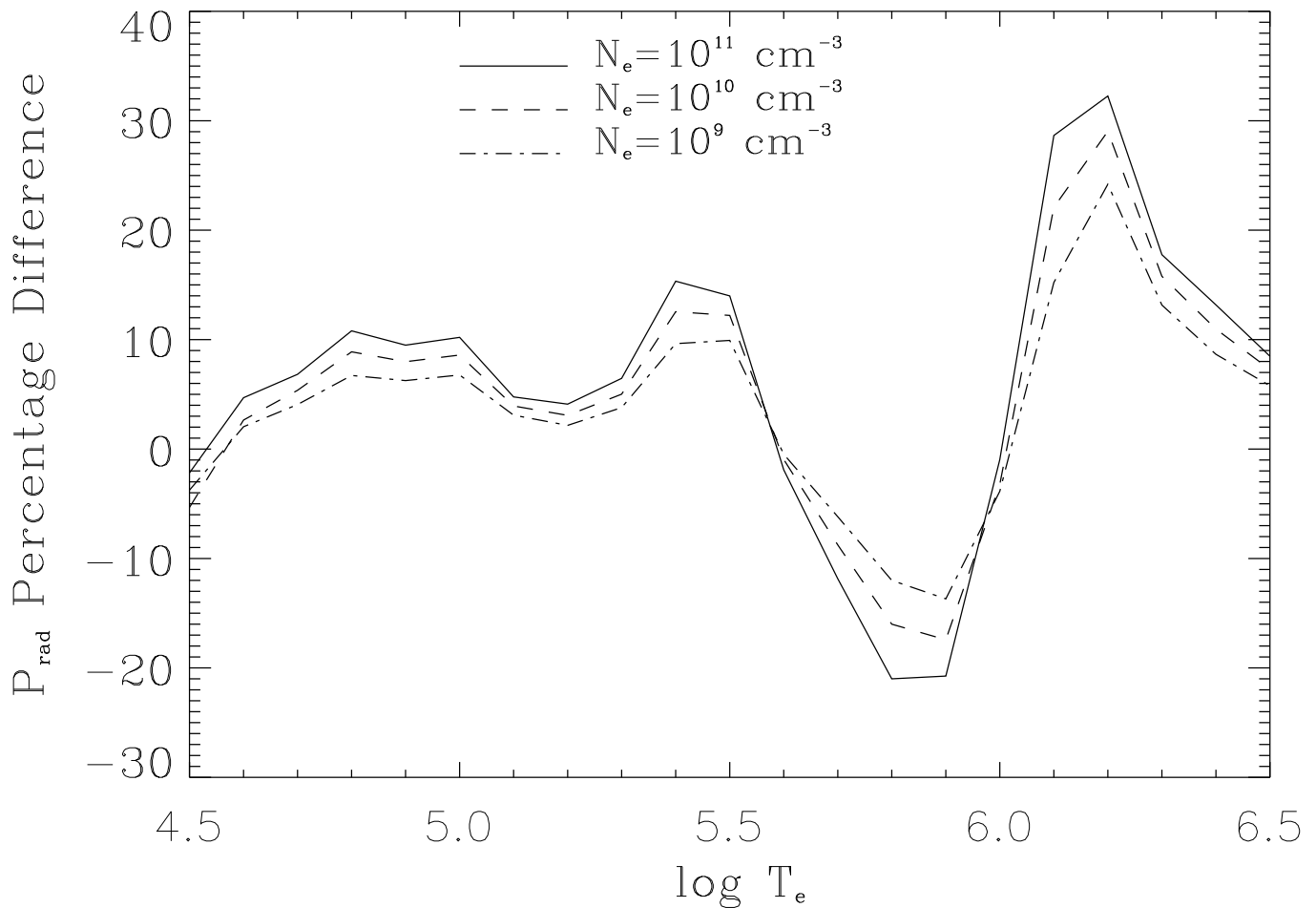


Fig. 2. The percentage difference in the radiative loss function assuming different electron densities: 10^6 versus 10^{11} cm^{-3} (solid line), 10^6 versus 10^{10} cm^{-3} (dashed line), 10^6 versus 10^9 cm^{-3} (dot-dash line).

although the difference is less than 20% compared to the low-density approximation.

Acknowledgements. Research at the Armagh Observatory is grant-aided by the N. Ireland Dept. of Culture, Arts and Leisure. This work was funded in part by a PRTL research grant for Grid-enabled Computational Physics of Natural Phenomena (Cosmogrid), plus PPARC Visitors grant PPA/V/S/2003/00049.

Vernazza, J.E. & Raymond, J.C., 1979, ApJ 228, L89
 Young, P.R., Del Zanna, G., Landi, E., Dere, K.P., Mason, H.E. & Landini, M., 2003, ApJS 144, 135

References

- Bates, D.R., Kingston, A.E. & McWhirter, R.W.P., 1962, Proc. Roy. Soc., A267, 297
 Burgess, A. & Summers, H.P., 1969, ApJ 157, 1007
 Del Zanna, G., Landini, M. & Mason, H.E., 2002, A&A 385, 968
 Doyle, J.G. & Raymond, 1984, Sol Phys, 90, 97
 Landi, E. & Landini, M., 1999, A&A 347, 401
 Lanzafame, A.C., Brooks, D.H., Lang, J., Summers, H.P., Thomas, R.J. & Thompson, A.M., 2002, A&A 384, 242
 Raymond, J.C. & Doyle, J.G., 1981, ApJ 245, 1141
 Summers, H.P. & Hooper, M.B., 1983, Plasma Physics, 25, 1311
 Summers, H.P., 2004 *The ADAS User Manual, version 2.6*, <http://adas.phys.strath.ac.uk>